

Modeling and Analysis of the Compatibility of Poly(ethylene oxide)/Poly(methyl methacrylate) Blends with Surface and Shear Inducing Effects

Dan Mu,¹ Jian-Quan Li,² Song Wang³

¹Department of Chemistry and Chemical Engineering, Zaozhuang University, Shandong 277160, China

²Physics and Electronic Engineering Department, Zaozhuang University, Shandong 277160, China

³Institute of Theoretical Chemistry, State Key Laboratory of Theoretical and Computational Chemistry, Jilin University, Changchun 130023, China

Received 12 April 2010; accepted 23 November 2010

DOI 10.1002/app.33820

Published online 19 April 2011 in Wiley Online Library (wileyonlinelibrary.com).

ABSTRACT: The compatibility of poly(ethylene oxide) (PEO) and poly(methyl methacrylate) (PMMA) blends was studied over a wide range of compositions at 400 K by mesoscopic modeling. Sixteen patterned surfaces of four types were designed and designated as “ci,” “co,” “gra,” and “rg” to study their influence on changing the microscopic phase morphology. The topography of the “ci” series surfaces was shaped by semicircular balls. Different radii were applied to simulate different degrees of surface roughness. The “co” series were composed of cubic columns as the mask, and the cubic columns were separated by equal spaces. Various sizes and heights of columns were used to simulate different degrees of surface roughness. The “gra” series were composed of surfaces with different areas of section and the same height to simulate different degrees

of surface roughness. The “rg” series were composed of concentric cuboids with continuous increasing heights and sizes. The “co” series surfaces were the most efficient distribution in changing the microscopic phase morphology, the “gra” and “rg” series surfaces were both the secondary, and the “ci” series surfaces placed the last. The results show that the effect of inducing surfaces depended on both the pattern of surfaces and the compositions of the blends. The shear effect was effective in changing the phase morphology, but its influencing effect depended on not only the shear rate, but also the compositions of the blends, especially when the blends were rich in PEO. © 2011 Wiley Periodicals, Inc. *J Appl Polym Sci* 122: 64–75, 2011

Key words: blending; calculations; computer modeling

INTRODUCTION

Poly(ethylene oxide) (PEO) and poly(methyl methacrylate) (PMMA) are both important polymers for synthesis and applications in a variety of engineering and biomedical areas.^{1–3} The study of PEO/PMMA blends is of interest because of the semicrystalline nature of PEO, the weak interactions between these two polymers, and their great difference in the glass transition temperatures (T_g), which make such blends a complex system. PEO/PMMA blends are miscible at a low temperature while they demonstrate to be immiscible at a high temperature such as 400 K,⁴ which is consistent with the experimental results of Fernandes et al.⁵ Several experimental results show that when microscopic or mesoscopic

morphology of polymers possesses regular distribution, the properties of these polymers are different from ordinary ones; thus they may be useful in engineering and polymer industry.^{6–8} However, there haven't been any reports about the inducing effects of patterned surfaces on the PEO/PMMA blends system, whose plain blends are immiscible at 400 K. Some inspiring results were obtained in this work, which can be applied to surface-fabrication to improve the function of surface-materials.

Meso-scale structures are of utmost importance during the production processes of many areas, such as polymer blends, block copolymer systems, surfactant aggregates in detergent materials, latex particles, and drug delivery systems. Mesoscopic dynamics models have been receiving increasing attention as they form a bridge between studies of micro-scale and macro-scale properties.^{9–12} Mesoscopic dynamics (MesoDyn)^{13,14} and dissipative particle dynamics (DPD) methods^{15,16} both treat the polymer chain at a mesoscopic level by grouping atoms together and then coarse-graining them to be persistent length polymer chains. These two mesoscopic modeling methods increase the simulation scale by several orders of magnitude compared with atomistic simulation methods. MesoDyn deals with the dynamic

Correspondence to: D. Mu (mudanjlu1980@yahoo.com.cn).

Contract grant sponsors: The project is supported by the Science-Technology Foundation for Middle-aged and Young Scientist of Shandong Province (BS2010CL048), Shandong Province Higher School Science & Technology Fund Planning Project (J10LA61) and Zaozhuang Scientific and Technological Project (200924-2).

mean-field density functional theory (DFT) in which the dynamics of phase separation can be described by Langevin-type equations to investigate polymer diffusion. The thermodynamic forces are found via mean-field DFT taking the Gaussian chain as a model. The most important molecular parameter is the “incompatibility parameter” χN , where χ is the Flory-Huggins interaction parameter and N is the degree of polymerization. However, owing to the soft interaction potential of the DPD method, it is not suitable for our work, especially in dealing with the interaction between blending materials and surfaces. Furthermore, in the study of the compatibility of PEO/PMMA blends in our former work, the MesoDyn simulation method was successfully applied to detect the phase morphologies of PEO/PMMA blends. From a theoretical point of view, these results clarified several conflicting conclusions of different experiments.⁴ Therefore, the MesoDyn method has been shown to be reliable when dealing with PEO/PMMA blends.

COMPUTATIONAL DETAILS

All calculations presented in this article were carried out by commercial software, Materials Studios, provided by Accelrys Company, running on an SGI work station. The MesoDyn module was used to study the microscopic phase morphology of PEO/PMMA blends at 400 K. This article consists of three parts: the first part is the study on the effect of inducing surfaces on microscopic morphology of PEO/PMMA blends; the inducing surfaces here are defined to study the inducing effect of the designed patterned surface. The second part is the research on shear effect on the basis of the first part; the third part is the study on the effect of shear rate on the basis of the second part.

Mesoscopic simulations included different PEO/PMMA blending compositions, 1/1, 1/2, 1/3, 1/4, 1/6, 2/1, 3/1, 4/1, 6/1, and 8/1 in molar ratio, roughly covering the whole composition range, and the polymer molecular weight distribution assumed with a polydispersity of 1. Ten blending models are given in Table I in detail. The molar ratio of PEO to PMMA, the weight percentages of PMMA, the density, and the input parameters of MesoDyn at 400 K⁴ are also listed in this table. The order parameter, denoted as P , is defined as the volume average of the difference between local density squared and the overall density squared, given by the equation^{4,17}

$$P_i = \frac{1}{V} \int_{\phi_i} [\eta_{\phi_i}^2(r) - \eta_{\phi_i}^2] dr$$

where η_i is dimensionless density (volume fraction) for species i . The larger the value of the order

TABLE I
Details of PEO/PMMA Blending Models and Their Input Parameters of MesoDyn at 400 K

Number	Symbol (molar ratio)	wt % of PMMA	P (g cm ⁻³)	Input parameter
1	1/6	93.16	1.1873	0.00266
2	1/4	90.09	1.1870	0.00217
3	1/3	87.20	1.1867	0.00243
4	1/2	81.96	1.1862	0.00197
5	1/1	69.43	1.1849	0.00184
6	2/1	53.18	1.1833	0.00636
7	3/1	43.09	1.1823	0.00217
8	4/1	36.22	1.1816	0.00878
9	6/1	27.46	1.1807	0.01094
10	8/1	22.11	1.1802	0.00217

parameter is, the more obvious the phase separation is. A decrease in P indicates better compatibility or miscibility, and the polymer phases mix more randomly.

To discuss the influencing effect, it is necessary to define a new parameter to describe it. The PEO/PMMA plain blends were set as reference cases and their order parameter values were named as “A.” In addition, the order parameter values of PEO/PMMA blends with the same composition induced by exotic influencing factors, such as surfaces or shear effect, were named as “B.” The values of $(B - A)/A$ were defined as variation rates of order parameters (VROP for abbreviation). By comparing the VROP values, effective inducing surfaces in changing the microscopic morphology of polymer blends with the same composition can be found. Compositions of polymer blends suffer the most with the same exotic influencing factor can also be found.

Surface inducing effect

Four different types of patterned surfaces set as substrates with inducing effect were designed and designated as “ci,” “co,” “gra,” and “rg” types to study which type of surfaces can induce vigorous phase separation of the PEO/PMMA blends, and the surfaces can be considered as the preferential wetting surfaces. The topography of the “ci” series surfaces was shaped by semicircular balls. Different radii were applied to simulate different degrees of surface roughness. The “co” series were composed of cubic columns as the mask, and the cubic columns were separated by equal spaces. Various sizes and heights of columns were used to simulate different degrees of surface roughness. The “gra” series were composed of surfaces with different areas of section and the same height to simulate different degrees of surface roughness. Furthermore, asymmetric surfaces such as gra-444 and gra-888, and the symmetric surfaces such as gra-2(444), gra-2(448) and gra-2(888) were built. The “rg” series were composed of

TABLE II
Mesoscopic Simulations of PS/PMMA Blends Induced by "ci," "co," "gra," "rg"
Type Surfaces

"ci" type	Row number (X -axis)	Row number (Y -axis)	Radius (nm)
ci-444	4	4	4
ci-882	8	8	2
"co" type	E/T^g (X -axis)	E/T^g (Y -axis)	Height (nm)
co-444	2/4	2/4	4
co-448	2/4	2/4	8
co-4412	2/4	2/4	12
co-884	4/8	4/8	4
co-888	4/8	4/8	8
co-8812	4/8	4/8	12
"gra" type	Row number (X -axis)	Height (nm)	S^f in X -axis
gra-444	4	4,3,2,1	N ^a
gra-888	8	8,7,6,5,4,3,2,1	N ^a
gra-2(444)	8	4,3,2,1,1,2,3,4	Y ^b
gra-2(448)	8	8,4,2,1,1,2,4,8	Y ^b
gra-2(888)	16	8,7,6,5,4,3,2,11,2,3,4,5,6,7,8	Y ^b
"rg" type	Layer number	Height (nm)	S^f (X & Y -axis)
rg-442	2	2,4	Y ^b
rg-884	4	8,4,2,1	Y ^b
rg-16168	8	16,14,12,10,8,6,4,2	Y ^b

^g the abbreviation of "effective/total row number"; ^f the abbreviation of "symmetry"; ^a means "No"; ^b means "Yes."

concentric cuboids with continuous increasing heights and sizes. The details about these four types of designed surfaces are listed in Table II. The 16 designs are visualized in Figure 1.

Result and discussion

These four types, "ci," "co," "gra," and "rg" series surfaces are further divided into six kinds, which are "ci," "co-4xx," "co-8xx," "gra-xxx," "gra-2(xxx)," and "rg-xxx." Figure 2 shows the VROP values of PEO/PMMA blends with inducing effects of these 16 surfaces. In addition, representative isodensity surfaces of 10 PEO/PMMA blends at 400 K are selectively demonstrated above and below the plotting of VROP values versus the volume fraction of PEO. Several features can be seen in the figure as follows:

1. In the subfigure showing the "ci" series surfaces, all the 10 PEO/PMMA blends demonstrate a relationship of $VROP_{ci-444} > VROP_{ci-882}$, which reveals that the PEO/PMMA blends showed a little more serious phase separation on rougher surfaces. It can be assumed that the degree of surface roughness of such "ci" series surfaces plays a small role in changing the microscopic phase morphology of PEO/PMMA blends. Moreover, there exists an order of $VROP_{8/1} > VROP_{6/1} > VROP_{4/1} > VROP_{3/1}$, which means that the phase-separating degree became much more intensive with the increase

in PEO content when the blends were rich in PEO. On the contrary, there is no obvious trend in PMMA-rich blends. From both the VROP values and their isodensity surface pictures, it can be seen that the 1/3 blends experienced the strongest phase separation.

2. In the subfigure showing "co" series surfaces, it can be seen first that the VROP curves of "co-4xx" and "co-8xx" are nearly the same in PMMA-rich blends, which means that the degree of surface roughness of such "co" type surfaces plays a small role in changing the microscopic phase morphology of PEO/PMMA blends while the co-4412 surface showed an exception especially in PMMA-rich blends. On the contrary, to some degree the effects of "co-4xx" and "co-8xx" surfaces on the phase morphology were different. The orders of VROP values are $VROP_{co-4412} > VROP_{co-448} > VROP_{co-444}$ for the "co-4xx" surfaces and $VROP_{co-888} > VROP_{co-884} > VROP_{co-8812}$ for the "co-8xx" surfaces. Second, in PEO-rich blends, the differences among VROP value curves for "co-4xx" surfaces are smaller than those for "co-8xx" surfaces, which mean that the higher the column height on smoother surface is, the more phase separation it can induce. On the contrary, the variation in column height of "co-4xx" surfaces plays a smaller role in changing the microscopic phase morphology of PEO/PMMA blends.

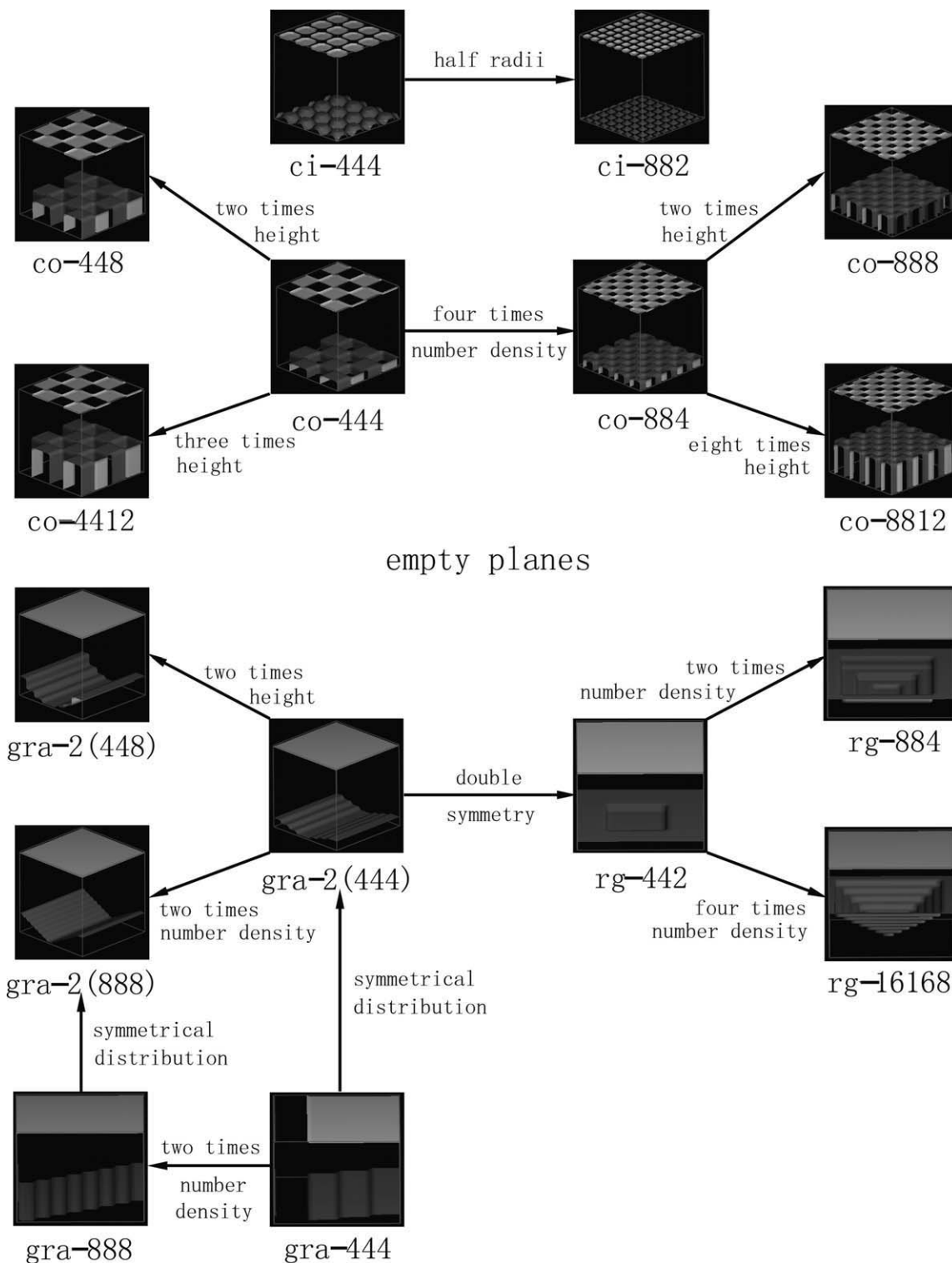


Figure 1 Illustration of four types of surfaces (“ci,” “rg,” “gra,” and “co” series) and the relationships among them.

3. In the subfigure showing the “gra” series surfaces, first it can be seen that the curves of “gra-xxx” are different from each other, which is the result from the differences in the degree of surface roughness. From the differences between the VROP value curves of gra-888 and gra-444, it is deduced that the inducing effect

of such “gra-xxx” surfaces on changing the microscopic phase morphology of blends depended on the degree of surface roughness. However, when a surface becomes more symmetrical, such as gra-2(888), its VROP value curve is nearly the same as that of gra-888, meaning that such smoother inducing surfaces

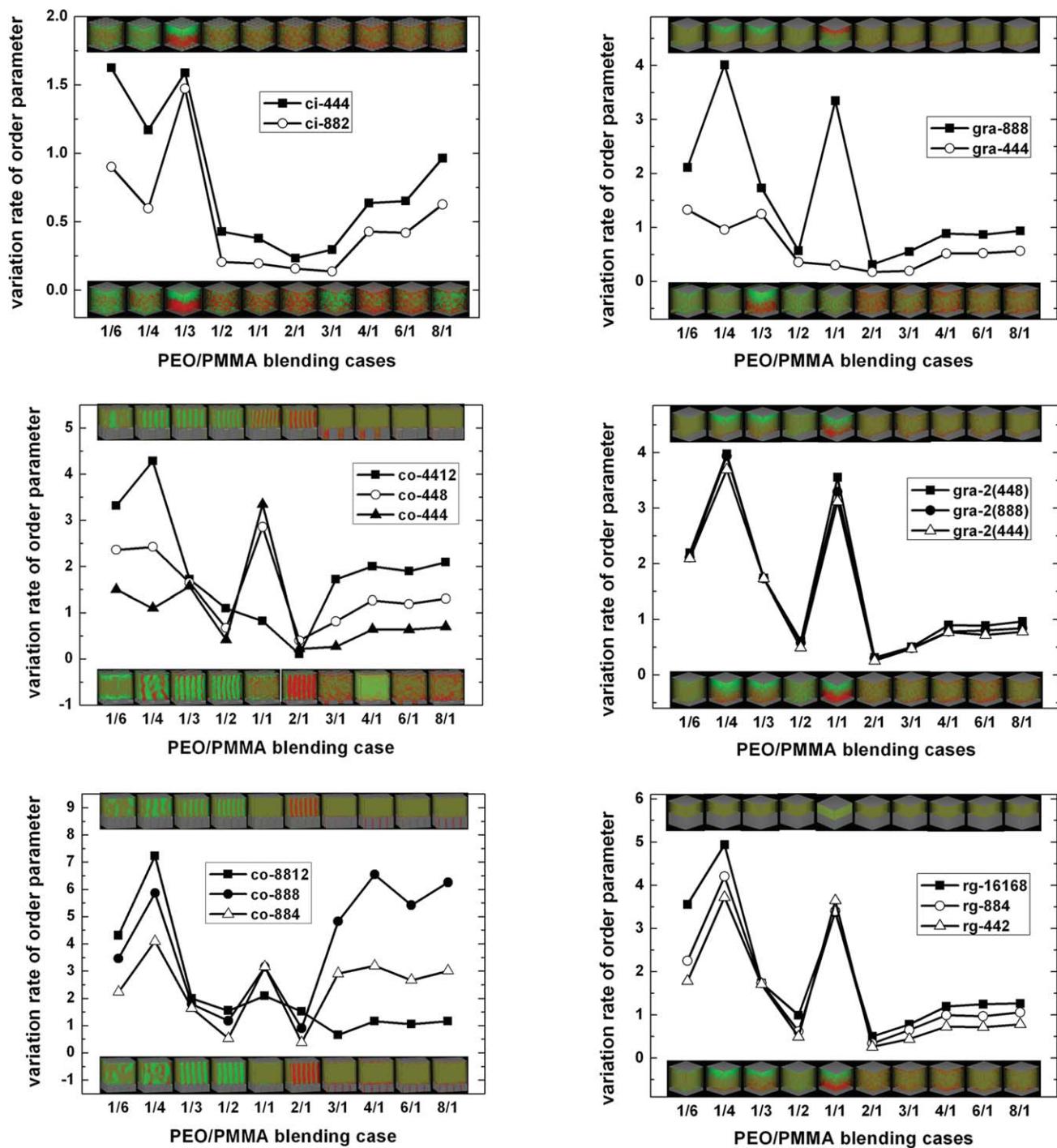


Figure 2 VROP values of 16 inducing surfaces versus 10 blending cases. The order in X axis is according to the increase in the volume fraction of PEO. Red represents PEO; green PMMA. There are ci-444 (top) and ci-882 (bottom) in “ci” graph, co-4412 (top), and co-444 (bottom) in “co-xx” graph, co-8812 (top), and co-888 (bottom) in “co-8xx” graph, gra-888 (top), and gra-444 (bottom) in “gra-xxx” graph, gra-2(448) (top) and gra-2(444) (bottom) in “gra-2(xxx)” graph, rg-16168 (top) and rg-442 (bottom) in “rg” graph. [Color figure can be viewed in the online issue, which is available at www.interscience.wiley.com.]

of “gra” series had the same effect on changing the microscopic phase morphology of PEO/PMMA blends no matter what degrees of symmetry of surfaces being used. Second, the VROP value curve is different from the curve

of gra-444, but nearly the same as that of gra-2(888), which means that the inducing effect of such rougher surfaces depended on the symmetrical distribution. Furthermore, when its symmetry was increased to some degree, the

VROP curve did not have more obvious changes, which is why the VROP curves of gra-2(448), gra-2(888) and gra-2(444) are nearly the same.

- In the subfigure showing the "rg" series surfaces, the VROP curves are similar to the curves of "gra-2(xxx)" series. The "rg" series surfaces were originated from "gra-2(xxx)" series surfaces essentially, so the degrees of symmetry of the former were twice that the latter. Therefore, this is a supplement result to prove the reasoning mentioned above that the degree of symmetry of smoother inducing surfaces can only influence the microscopic phase morphology in a certain range; the VROP curves of the surfaces will have little change upon increasing of the degree of symmetry when it reaches a certain value. Furthermore, the degree of surface roughness of "rg" series surfaces plays a great role in changing the microscopic phase morphology of PEO/PMMA blends, which were rich in either PEO or PMMA. In the six subfigures of Figure 2, the VROP values of different series surfaces show an order of $VROP_{co} > VROP_{gra} \sim VROP_{rg} > VROP_{ci}$ approximately. These results offer different clues in how to change the microscopic phase morphology of PEO/PMMA blends.

According to the outstanding differences shown in Figure 2, 1/4, 1/1, and 4/1 blends were chosen as three representative blending cases. Figures 3–5 display the mesoscopic simulation results of 1/4 (rich in PMMA), 1/1 (rich in PMMA), and 4/1 (rich in PEO) blends cases, respectively. There are several outstanding features in their VROP values and one of which is the transition in phase morphology. The initial plain PEO/PMMA blends were miscible, but they demonstrated local phase separation due to the inducing effect of surfaces, especially the "co" series inducing surfaces. It is shown that it was much easier to obtain more ordered phase separation morphologies in 1/4 blends than in 1/1 and 4/1 blends, which resulted from the difference in diffusion coefficient between PEO and PMMA components.¹⁸

Shear effect on the basis of surface inducing effect

To stabilize the numerical calculation, the time step for MesoDyn calculation, τ , was chosen as 50 ns, and the total simulation time was 20 ms for every blending case. The noise parameter value of 75.002 by default was used for the numerical speed and stability. The adopted grid dimensions were $32 \times 32 \times 32 \text{ nm}^3$, and the size of the mesh over which density variations were to be plotted in MesoDyn length unit was 1 nm.

Result and discussion on the order parameter

The shear rate was set to 0.001 ns^{-1} to study the effect of shear effect on the microscopic phase morphology. The following simulations were on the basis of PEO/PMMA blends induced by surfaces. Figure 6 shows the plots of the values of order parameter versus compositions of 10 blend cases with 16 inducing surfaces. Several obvious features can be seen as follows:

- For the PMMA-rich blends, such as 1/6, 1/4, 1/3, and 1/2 blends, the change tendencies of order parameter values are nearly the same in an increasing trend. In addition, the differences in order parameter values of 16 lines with the same composition are very small. These indicate that different inducing surfaces nearly had the same effect in changing the microscopic morphologies for PMMA-rich blends, but the composition of blends was the decisive factor. Furthermore, the microscopic morphology showed a big change when blends were rich in PEO component.
- For the blends of middle two cases, such as 1/2 and 1/1 blends, the transition trends from 1/2 to 1/1 with various surfaces induced are different, which are upward in co-4412, co-448, co-8812, gra-2(448), rg-884, and rg-16168 cases, while those in other cases are downward. These indicate that the same shear rate had different influencing effects depending on the degree of roughness of these four types of surfaces. The rougher the surface was, the more ordered phase morphology would appear.
- For the blends had roughly equal PEO and PMMA contents, such as 1/1 and 2/1 blends, these 16 lines in the figure are in an ascending trend, which indicates that with all kinds of inducing surfaces more ordered phase morphology would appear under shear stress with the increase in PEO volume fraction.
- For PEO-rich blends, such as 3/1, 4/1, 6/1, and 8/1 blends, the transition trends of the order parameter values are similarly with four or three crossing points. The slopes of these 16 lines are listed in Table III. The order of slopes is $P_{co-4412} > P_{co-8812} > P_{rg-16168} > P_{gra-2(448)} > P_{co-888} > P_{co-448} > P_{rg-884} > P_{gra-2(888)} > P_{gra-888} > P_{gra-2(444)} > P_{co-444} > P_{co-884} > P_{gra-444} > P_{ci-444} > P_{rg-442} > P_{ci-882}$ with the last four slopes being negative value, which means shear stress caused these four phase morphologies less ordered with the increase in PEO, while it exerted a reinforcing effect on the other twelve cases.

To make it clearer, the order above can be divided into six groups according to six kinds of inducing surfaces. In the "ci" series surfaces, the order of the

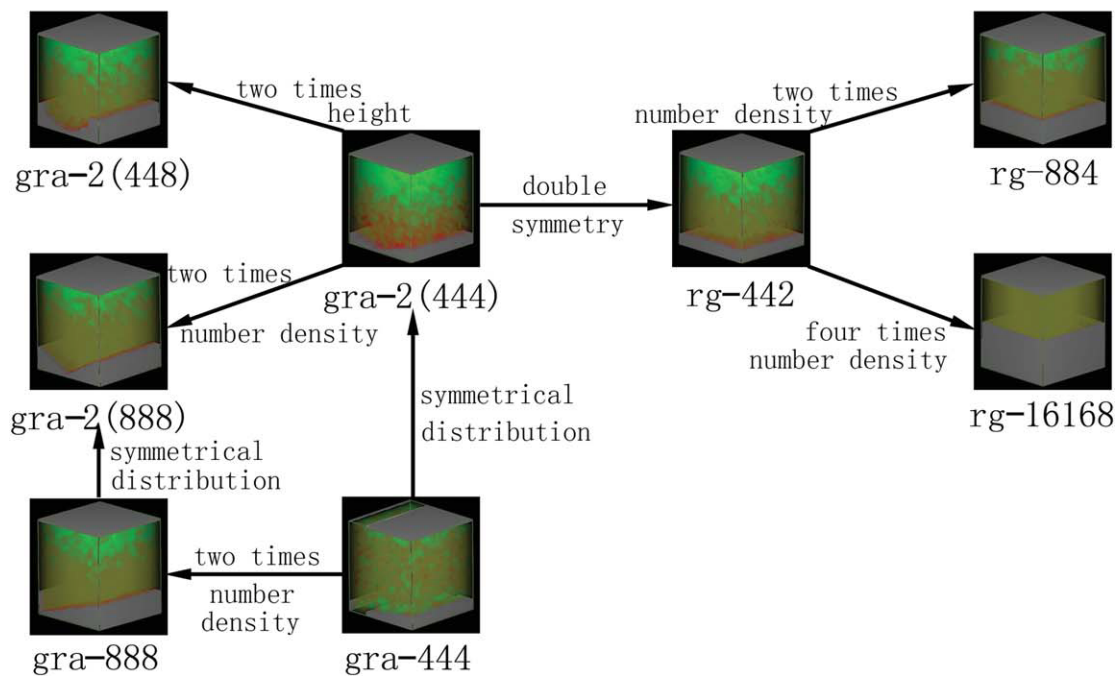
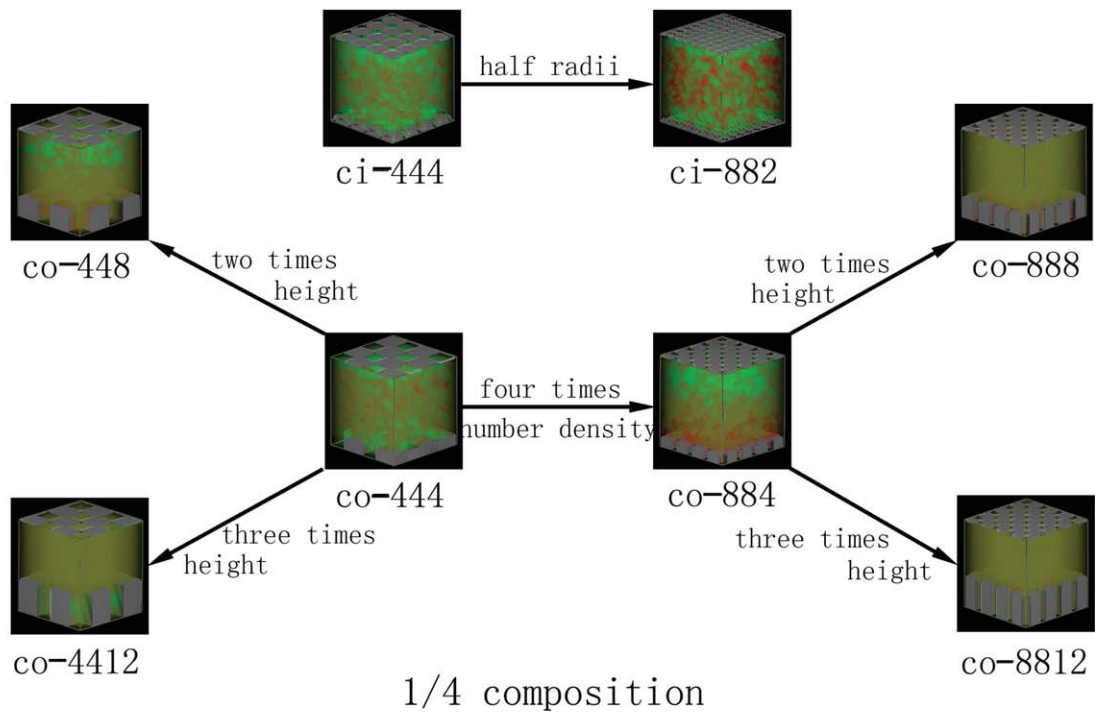


Figure 3 Iso-density surfaces of PEO/PMMA blends induced by 16 surfaces. The PEO volume fraction is 10.21% (1/4 blends), rich in PMMA. Red represents PEO; green PMMA. [Color figure can be viewed in the online issue, which is available at wileyonlinelibrary.com.]

parameter values is $P_{ci-444} > P_{ci-882}$ and they are both negative; in the “co-4xx” series surfaces, the order of the parameter values is $P_{co-4412} > P_{co-448} > P_{co-444}$; in the “co-8xx” series surfaces, the order of the parameter values is $P_{co-8812} > P_{co-888} > P_{co-884}$; in the “gra-xxx” series surfaces, the order is $P_{gra-888} >$

$P_{gra-444}$, and the latter is negative; in the “gra-2(xxx)” series surfaces, the order of the parameter values is $P_{gra-2(448)} > P_{gra-2(888)} > P_{gra-2(444)}$; in the “rg-xxx” series surfaces, the order is $P_{rg-16168} > P_{rg-884} > P_{rg-442}$ and the last is negative. In addition, two more relationships, $P_{gra-2(888)} > P_{gra-888}$ and $P_{gra-2(444)} >$

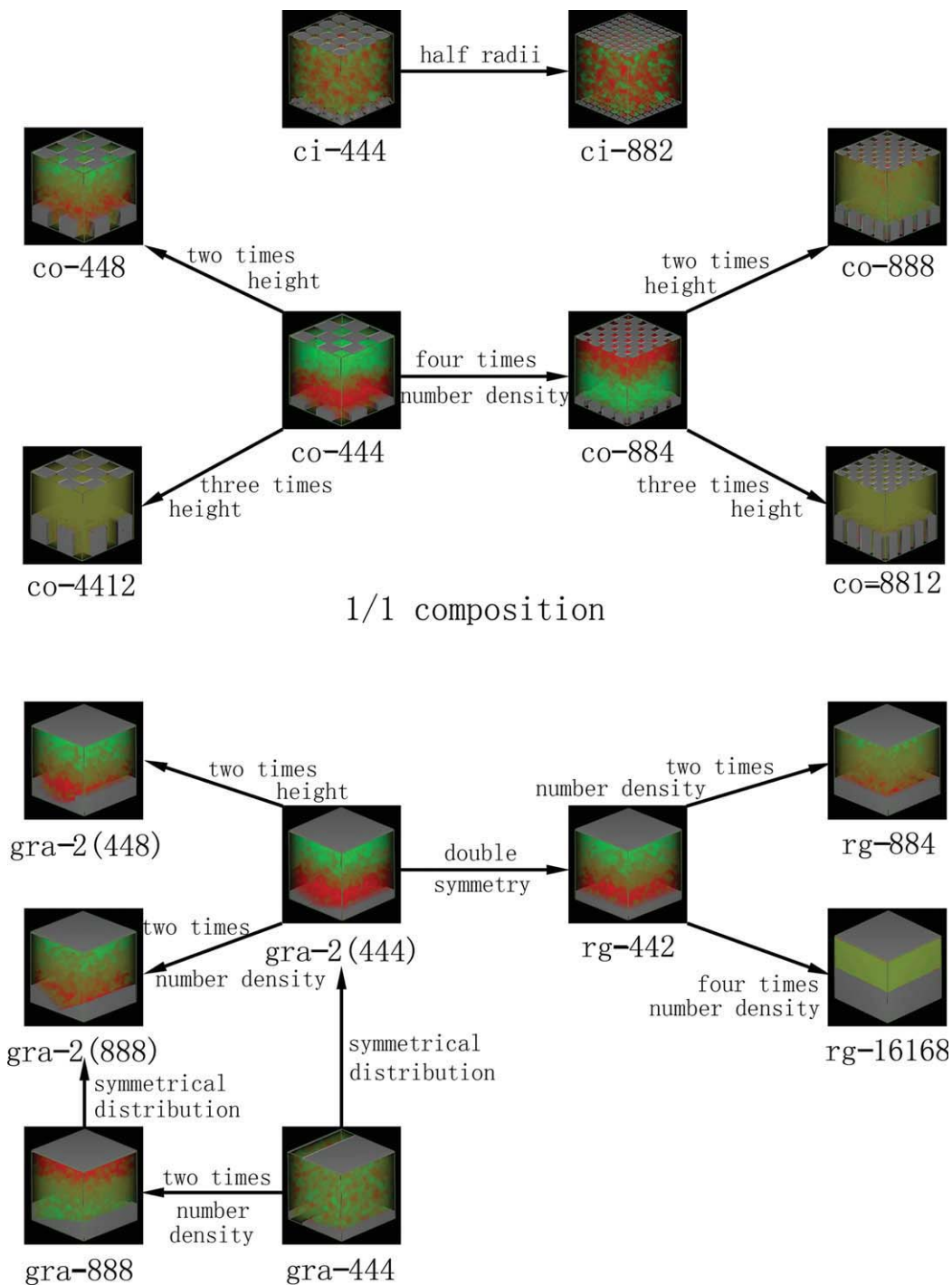


Figure 4 Iso-density surfaces of PEO/PMMA blends induced by 16 surfaces. The PEO volume fraction is 31.26% (1/1 blends), rich in PMMA. Red represents PEO; green PMMA. [Color figure can be viewed in the online issue, which is available at wileyonlinelibrary.com.]

$P_{\text{gra-444}}$ can be seen. From these eight relationships mentioned above we can deduce that the shear effect had an obvious influence on the order of phase morphology when there were more influencing factors on the inducing surfaces, such as more columns, obvious increase in distance between columns, and so on.

Result and discussion on the VROP data

Figure 7 shows the shear effect on changing the phase morphology of blends with surface induced. Several features can be seen as follows:

1. The changing trend in Figure 7 is nearly the same as it in Figure 6 except that the 1/2 to 1/

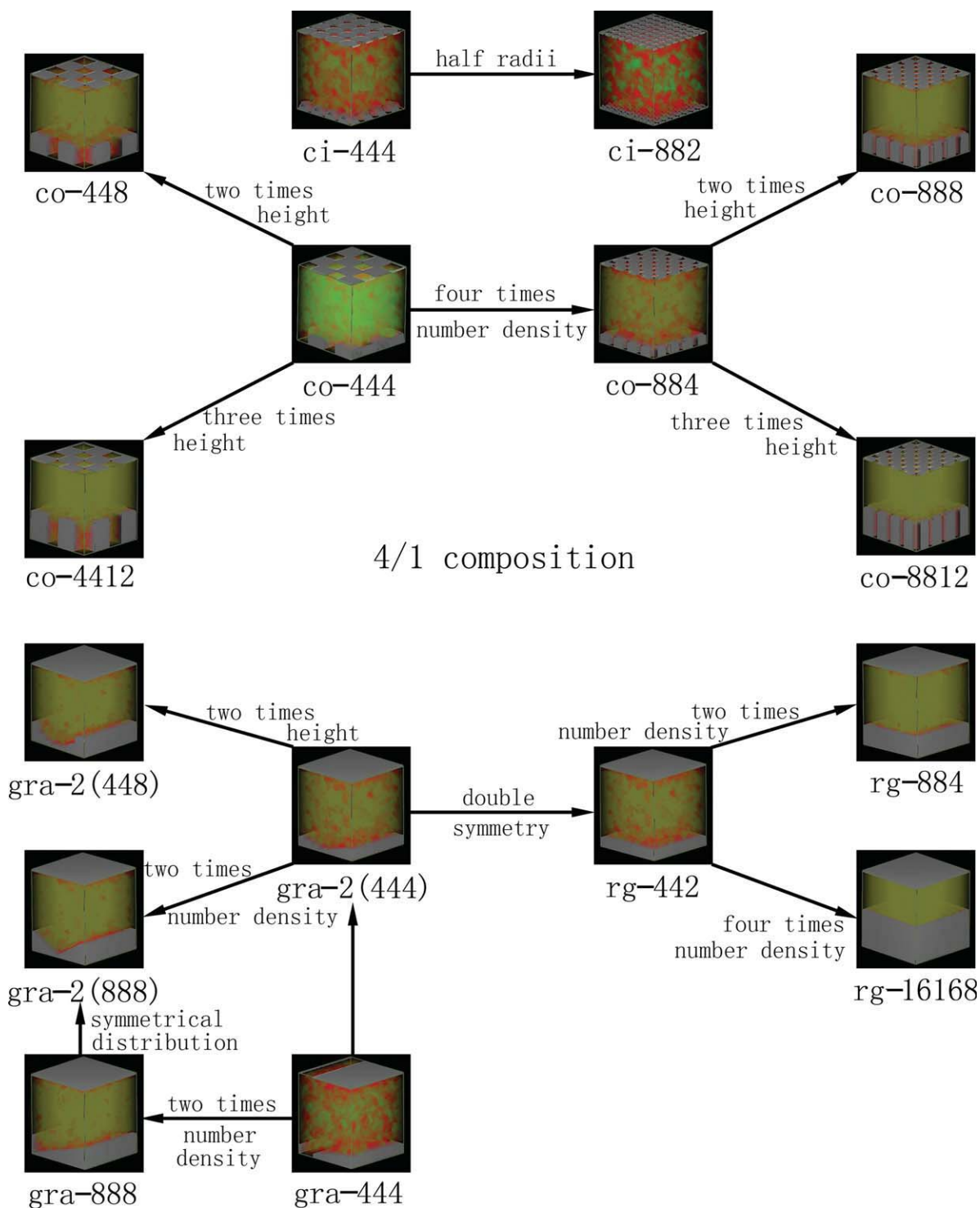


Figure 5 Iso-density surfaces of PEO/PMMA blends induced by 16 surfaces. The PEO volume fraction is 64.53% (4/1 blends), rich in PEO. Red represents PEO; green PMMA. [Color figure can be viewed in the online issue, which is available at wileyonlinelibrary.com.]

- 1 blends' slopes are either positive or negative, and the corresponding point is considered as a turning point.
2. The VROP values of 16 lines for PEO-rich blends, such as 4/1, 6/1, and 8/1 blends, rise very rapidly and these three points of 16 lines all converge one

line approximately, which is also the same as that in Figure 6. Furthermore, we also can deduce other VROP values of PEO-rich blends from such slope data. These 16 slopes are listed in Table IV, and the order of slopes is $VROP_{co-4412} > VROP_{co-8812} > VROP_{rg-16168} > VROP_{gra-2(448)} >$

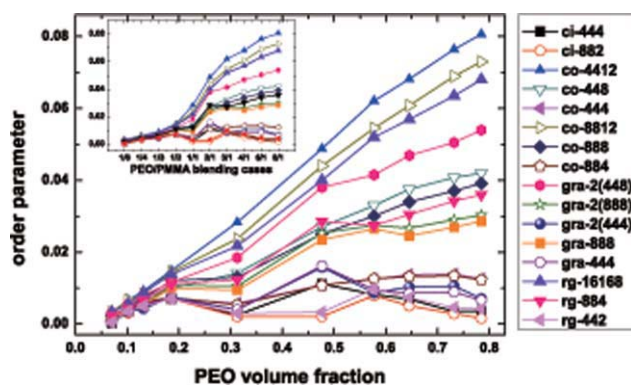


Figure 6 The order parameter values of 10 representative blends with both surfaces and 0.001 ns^{-1} shear induced. [Color figure can be viewed in the online issue, which is available at wileyonlinelibrary.com.]

$$\begin{aligned} \text{VROP}_{\text{co-888}} &> \text{VROP}_{\text{rg-884}} > \text{VROP}_{\text{gra-2(888)}} > \\ \text{VROP}_{\text{gra-888}} &> \text{VROP}_{\text{co-444}} > \text{VROP}_{\text{co-884}} > \\ \text{VROP}_{\text{gra-2(444)}} &> \text{VROP}_{\text{gra-444}} > \text{VROP}_{\text{rg-442}} > \\ \text{VROP}_{\text{ci-444}} &> \text{VROP}_{\text{ci-882}} > \text{VROP}_{\text{co-448}}. \end{aligned}$$

In addition, the slope of line corresponding to co-448 is nearly zero which shows little change in order parameter value with the increase in PEO. To make a clear comparison with the corresponding relations in the above part about the relations about the order parameter values, it is necessary to divide such long relation into six groups. It is shown that there exist the same relationships between VROP and the order parameter values of the five kinds of surfaces except the “co-4xx” series inducing surfaces: for the “co-4xx” series inducing surfaces there is an order of $\text{VROP}_{\text{co-4412}} > \text{VROP}_{\text{co-444}} > \text{VROP}_{\text{co-448}}$, which is different from the order of order parameter values, $P_{\text{co-4412}} > P_{\text{co-448}} > P_{\text{co-444}}$. The former demonstrates the influencing strength of shear effect on changing the phase morphology with surface induced, but the latter demonstrates the inducing result. Although the order parameter of “co-448” is high enough to prove its ability of producing much ordered phase morphology, the obvious low VROP value indicates

TABLE III
Slopes of Order Parameter Lines Consisting of 3/1, 4/1, 6/1, and 8/1 Blends

Symbol (inducing surfaces)	Slope data	Symbol (inducing surfaces)	Slope data
ci-444	-0.0254	gra-2(448)	0.0576
ci-882	-0.0299	gra-2(888)	0.0258
co-4412	0.0904	gra-2(444)	0.0115
co-448	0.0429	gra-888	0.0288
co-444	0.0090	gra-444	-0.0115
co-8812	0.0900	rg-16168	0.7682
co-888	0.0431	rg-884	0.0417
co-884	0.0057	rg-442	-0.0279

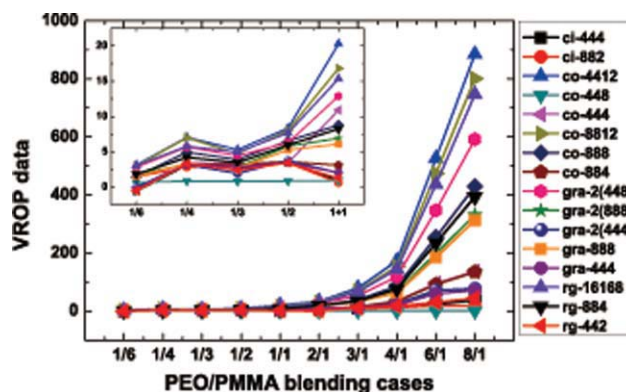


Figure 7 VROP values of 10 representative blends with both surfaces and 0.001 ns^{-1} shear induced on the basis of plain surface inducing. [Color figure can be viewed in the online issue, which is available at wileyonlinelibrary.com.]

shear effect exerted little influence on changing or improving the phase morphology of blends with the variation of PEO content.

Different shear rates on the basis of surface inducing effect

The results above show that the shear effect was effective in changing the phase morphology of blends; it even could induce the phase separation. Then shear rate was raised to 0.002 ns^{-1} , twice as that of the original one, and their VROP values are compared with those at a shear rate of 0.001 ns^{-1} .

RESULT AND DISCUSSION

Blends cases of 1/2 (PEO volume fraction 18.53%), 2/1 (PEO volume fraction 47.64%) and 8/1 (PEO volume fraction 78.44%) were used as examples of compositions rich in PMMA, roughly equal in PEO and PMMA, and rich in PEO, respectively. Figure 8 shows the VROP values of 1/2, 2/1 and 8/1 representative blends with 0.002 ns^{-1} shear inducing on

TABLE IV
Slopes of VROP Value Lines Consisting of 4/1, 6/1, and 8/1 Blends

Symbol (inducing surfaces)	Slope data	Symbol (inducing surfaces)	Slope data
ci-444	144.43	gra-2(448)	3326.60
ci-882	39.26	gra-2(888)	1862.90
co-4412	5014.52	gra-2(444)	388.97
co-448	0.06	gra-888	1769.56
co-444	735.92	gra-444	374.92
co-8812	4556.36	rg-16168	4232.37
co-888	2419.44	rg-884	2237.22
co-884	727.36	rg-442	189.63

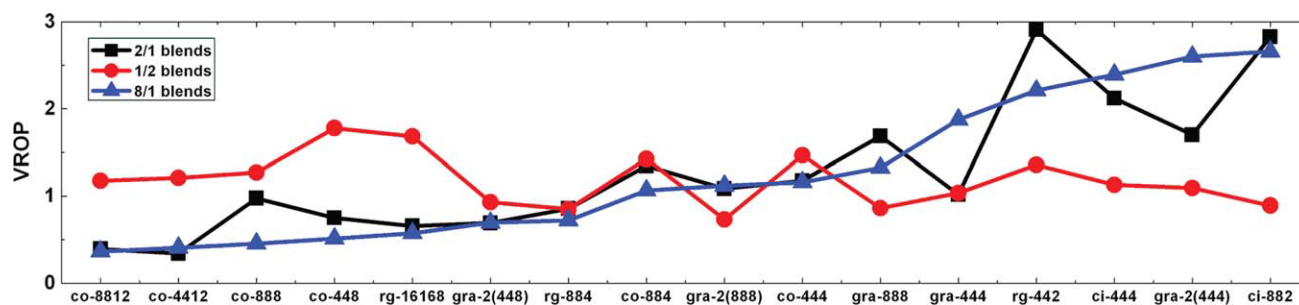


Figure 8 VROP values induced both by 16 surfaces and 0.002 ns^{-1} shear rate on the basis of 0.001 ns^{-1} inducing shear rate. [Color figure can be viewed in the online issue, which is available at wileyonlinelibrary.com.]

the basis of 0.001 ns^{-1} . Three obvious features are as follows:

1. The line of 8/1 blends is used as an example. The VROP values in details are as follows: in the "ci" series surfaces, the order is $VROP_{ci-444} < VROP_{ci-882}$; in the "co-4xx" series surfaces, the order is $VROP_{co-4412} < VROP_{co-448} < VROP_{co-444}$; in the "co-8xx" series surfaces, the order is $VROP_{co-8812} < VROP_{co-888} < VROP_{co-884}$; in the "gra-xxx" series surfaces, the order is $VROP_{gra-888} < VROP_{gra-444}$; in the "gra-2(xxx)" series surfaces, the order is $VROP_{gra-2(448)} < VROP_{gra-2(888)} < VROP_{gra-2(444)}$; in the "rg-xxx" series surfaces, the order is $VROP_{rg-16168} < VROP_{rg-884} < VROP_{rg-442}$. These six orders are exactly the opposite of the corresponding orders of those values at a 0.001 ns^{-1} shear rate induced on the basis of plain surfaces. These results show that though the shear effect is effective in changing the phase morphology, its influencing effect is weak for higher shear effect, derived from the comparison of VROP which is on the basis of lower shear inducing.
2. The 2/1 line varies around 8/1 line. It is deduced that when the blends consisted of equal contents of PEO and PMMA, its influencing effect was similar to that in the PEO-rich blends. It resulted from the difference in diffusion coefficients between PEO and PMMA components.¹⁸
3. The 1/2 line changes in a peculiar range and the types did not make a big difference in these values, which means that the surface and higher shear rate had limited influencing effect in changing the phase morphology in PMMA-rich blends.

CONCLUSIONS

Four different types of inducing surfaces were designed to study their inducing effect on changing the microscopic phase morphology of PEO/PMMA blends. The topography of the "ci" series surfaces was shaped by semicircular balls. Different radii were applied to simulate different degrees of surface

roughness. The "co" series were composed of cubic columns as the mask, and the cubic columns were separated by equal spaces. Various sizes and heights of columns were used to simulate different degrees of surface roughness. The "gra" series were composed of surfaces with different areas of section and the same height to simulate different degrees of surface roughness. The "rg" series were composed of concentric cuboids with continuous increasing heights and sizes. The "co" series surfaces were the most efficient distribution in changing the microscopic phase morphology, and the degree of surface roughness was a vital factor. The "gra" and "rg" series surfaces both had symmetrical distribution, and they had nearly the same influencing effect in changing the microscopic phase morphology of PEO/PMMA blends and tied for the second place in the order of influence. The last was the "ci" series surfaces in the order. There is an obvious relation between "gra" and "rg" series surfaces. When the inducing surfaces became smoother, the inducing effects of these surfaces would level off with the increase of its degree of symmetry. Furthermore, the degree of surface roughness was a less important factor in changing the microscopic phase morphology of PEO/PMMA blends.

Shear effect could change the phase morphology efficiently and even could induce phase separation. With the same 0.001 ns^{-1} shear rate, the rougher the inducing surfaces were, the more serious phase separating appeared. However, when the shear rate was increased to 0.002 ns^{-1} , its influencing effect became weaker. The shear effect combined with surface induced showed a significant influencing effect on the PEO-rich blends and the blends with equal contents of PEO and PMMA, but a limited effect on the PMMA-rich blends.

References

1. Seymour, R. B.; Carraher, C. E. *Polymer Chemistry*, 2nd ed.; Marcel Dekker: New York, 1988.
2. Munk, P.; Aminabhavi, T. M. *Introduction to Macromolecular Science*; Wiley-VCH: New York, 2002.
3. Carraher, C. E. *Giant Molecules: Essential Materials for Everyday Living and Problem Solving*, 2nd ed.; Wiley: New York, 2003.

4. Mu, D.; Huang, X. R.; Lu, Z. Y.; Sun, C. C. *Chem Phys* 2008, 348, 122.
5. Fernandes, A. C.; Barlow, J. W.; Paul, D. R. *J Appl Polym Sci* 1986, 32, 5481.
6. Ma, P. X.; Choi, J. W. *Tissue Eng* 2001, 7, 23.
7. Baumert, B.; Stratmann, M.; Rohwerder, M. *Mater Res Soc Symp Proc* 2004, 795, u5.23.1.
8. Ambrosio, A.; Alderighi, M.; Labardi, M.; Pardi, L.; Fuso, F.; Allegrini, M.; Nannizzi, S.; Pucci, A.; Ruggeri, G. *Nanotechnology* 2004, 15, S270.
9. Valls, O. T.; Farrell, J. E. *Phys Rev E* 1993, 47, R36.
10. Ramirez-Piscina, L.; Hernández-Machado, A.; Sancho, J. M. *Phys Rev B* 1993, 48, 125.
11. Kawakatsu, T.; Kawasaki, K.; Furusaka, M.; Okabayashi, H.; Kanaya, T. *J Chem Phys* 1993, 99, 8200.
12. Shinozak, A.; Oono, Y. *Phys Rev E* 1993, 48, 2622.
13. Fraaije, J. E. M. *J Chem Phys* 1993, 99, 9202.
14. Fraaije, J. G. E. M.; van Vlimmeren, B. A. C.; Maurits, N. M.; Postma, M.; Evers, O. A.; Hoffman, C.; Altevogt, P.; Goldbeck-Wood, G. *J Chem Phys* 1997, 106, 4260.
15. Groot, R. D.; Warren, P. B. *J Chem Phys* 1997, 107, 4423.
16. Groot, R. D.; Madden, T. J. *J Chem Phys* 1998, 108, 8713.
17. MesoDyn, *Materials Studio Online Help* 2006 Accelrys Software, Inc. All rights reserved.
18. Brandrup, J.; Immergut, E. H.; Grulke, E. A. *Polymer Handbook*; Wiley: New York, 1999.